Journal of Alloys and Compounds 513 (2012) 159–164

Contents lists available at SciVerse ScienceDirect

Journal of Alloys and Compounds

journal homepage: www.elsevier.com/locate/jallcom

A model for the decomposition of titanium hydride and magnesium hydride

Gelena Stepura*, Valery Rosenband, Alon Gany

Faculty of Aerospace Engineering, Technion, Israel Institute of Technology, Haifa 32000, Israel

ARTICLE INFO

Article history:
Received 17 October 2010
Received in revised form 3 October 2011
Accepted 4 October 2011
Available online 25 October 2011

Keywords:
Metal hydrides
Diffusion in solids
Phase transition
Hydride decomposition

ABSTRACT

This work presents a theoretical model of metal hydride particle decomposition with particular relation to titanium hydride and magnesium hydride. The model is based on the shrinking core approach, revealing the variation of major parameters such as temperature and hydrogen fraction with time. An experimental effort aimed at examining the theoretical model includes TGA–DTA tests of hydride particle decomposition in argon atmosphere. The model predictions reveal good agreement with the experiments.

1. Introduction

Metal hydrides have been investigated by many researchers since the 1960s. They are used in the mechanical and chemical industries due to their unique mechanical and thermodynamic properties [1,2]. Thermochemical calculations show that certain metal hydrides can improve the energetic performance of chemical propellants. Recently, the use of metal hydrides for hydrogen storage has become of major interest, offering compactness, safety, and ease of storage and transportation of hydrogen.

Among of the promising hydrides are titanium hydride and magnesium hydride, as well as their ternary compositions, which may exhibit better hydrogen desorption properties than binary hydrides of either magnesium or titanium [3]. Note, however, that hydrogenation rate of magnesium is slow, and the release of hydrogen from MgH_2 requires high temperatures [4]. Since metal hydrides are used in many modern technologies, the option of an inexpensive and fast production of them is very attractive. In the last two decades methods of mechanochemical synthesis [5–8] and of self-propagating high-temperature synthesis (SHS) [9–11] have been developed.

Metal hydride decomposition occurs usually as a result of heating of the hydride to a high temperature. Certain less stable hydrides (like aluminum hydride) may undergo some decomposition almost without heating. The chemical kinetics of metal hydride decomposition have been investigated, using different methods and techniques such as TGA (thermo gravimetric analysis), DSC (differential scanning callorimetry), TDS (thermal desorption spectrometry), TC (thermo cycling) [12], and others. Most of the known models for hydride decomposition consider hydrogen desorption as the rate controlling step of the decomposition process, which is different for every metal hydride. The main available models can be divided into three groups: "shrinking core" models, "nucleation and growth" models, and "multiple step" kinetics.

1.1. "Shrinking core" models

These models assume a simplified phase diagram of metal–hydrogen, including only two phases: a bulk of a hydride phase surrounded by a solid solution of hydrogen within the metal, containing a smaller concentration of hydrogen compared to the hydride phase core. The decomposition process is characterized by shrinkage of the hydride phase core region. The decomposition rate is calculated by the rate-determining step of the decomposition process among the following processes: diffusion of hydrogen within the hydride region, diffusion of hydrogen within the solid solution region, phase transformation from hydride to the solution, surface penetration of hydrogen atoms, surface recombination of hydrogen atoms into molecules, gas desorption. Models adopting this general scheme are presented, for instance, in [13–16]. The main advantages of this type of models are the relatively simple calculations involved and the good agreement with experimental results. A disadvantage of the "shrinking core" kinetic model is its inadequacy to predict decomposition rate for irregular sample shapes.

* Corresponding author. Tel.: +972 54 2002712.
E-mail address: gelena.stepura@gmail.com (G. Stepura).

0925-8388/$ – see front matter © 2011 Elsevier B.V. All rights reserved.
doi:10.1016/j.jallcom.2011.10.012

Nomenclature

C_β	hydrogen mass fraction in hydride core
C_α	hydrogen mass fraction in solid solution
$C_{\alpha m}$	maximum hydrogen mass fraction in solid solution
$\bar{C}_p$	average specific heat of particle
C_{p_ox}	specific heat of oxide
C_{p_α}	specific heat of solid solution
C_{p_β}	specific heat of hydride core
D	diffusion coefficient
D_0	diffusion coefficient constant
$\bar{d}$	particle average density
d_α	solid solution density
d_β	hydride core density
d_{ox}	oxide density
E	activation energy
f	function of heating
$H_{\beta\to\alpha}$	heat of phase transition from hydride to solid solution
$H_{\alpha\to M}$	heat of phase transition from solid solution to metal
$\dot{m}$	mass desorption rate of hydrogen
Ox	oxidizer
R	particle radius
r	radial coordinate
T	temperature
T_s	particle temperature
T_0	initial particle temperature
t	time
t_*	time of hydride core decomposition
t_{**}	time of final hydrogen desorption from the particle
W	molecular weight
Greek	
δ	thickness of oxide film
ρ	hydride core radius
$\Re$	universal gas constant

1.2. "Nucleation and growth (NG)" kinetic models

This type of modeling is based on a different view of the hydride particle behavior during decomposition: instead of a shrinking core, where the product is formed outside of the core region, the NG model assumes random nucleation and growth processes within the bulk, where the product is formed evenly within the particle volume. Such models are usually based on a direct dependence of decomposition rate on temperature (Arrhenius type parameter), and are presented by Avrami Yerofeev equations (e.g., in [17]) of different orders for two-phase reactions. The instantaneous decomposition rate is determined by the reacting fraction of the material, using a parameter n (known as Avrami parameter), which is sometimes defined as a number of nucleation/growth dimensions or the order of chemical reaction [18–20]. The NG model gives apparent global kinetics having to be calibrated by experiments.

1.3. "Multiple step" kinetics

This class of models includes several consecutive steps in the calculation of decomposition rate: hydride decomposition, phase transition, bulk diffusion, surface penetration, hydrogen atoms recombination, and final gas desorption. Calculating decomposition rate according to every step and comparing with experimental data determine the limiting step (or steps) of the reaction. Different groups of researchers applying this approach have used a different number of steps: Martin et al. [21] defined five intermediate stages, whereas Chou et al. [22] defined only one step (diffusion within the hydride region). Gondor and Lexcellent [23] presented two models: for a macro hydride sample (a group of particles) and for a micro sample (a single particle). The models were based on multiple step kinetics combined with evaluation of hydrogen absorption/desorption by modeling of pressure composition isotherm (PCI) or temperature composition isobar (TCI) curves. The first model included three steps (chemisorption, bulk diffusion, and phase transformation) and the second – five steps.

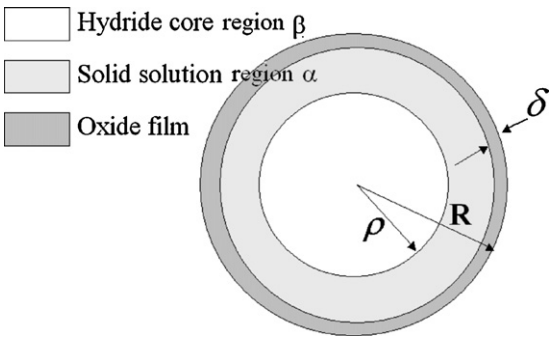

Fig. 1. Schematic illustration of a metal hydride particle during decomposition.

The above mentioned models refer to hydride decomposition without any chemical interaction with the ambience: i.e., decomposition under vacuum or in inert gas atmosphere. The proposed model refers to similar conditions. However, it accounts for the existence of an initial oxide layer around the particles, and the resulting hydrogen diffusion through it. The assumption of natural oxide film presence corresponds to investigations of different metal hydrides (e.g., hydrides of titanium, magnesium, lithium and zirconium) [24–27]. Several works [28–30] reveal that the diffusion coefficient of hydrogen through a titanium oxide film is smaller by a few orders of magnitude than diffusion coefficients of hydrogen within titanium hydride or titanium–hydrogen solid solution. For slow heating regime, like in TGA, one may assume that diffusion of hydrogen through the oxide layer is the rate determining step of hydride decomposition, whereas hydrogen concentration gradients within the other regions of the particle are negligible. Experimental work with corresponding conclusions is presented by [31,32].

1.4. Objectives

The present research studies metal hydride decomposition. Its main objective is to develop a theoretical model for decomposition of metal hydride particles in inert atmosphere or vacuum and to compare the prediction to experimental results. In particular, the study deals with decomposition of titanium hydride and magnesium hydride under heating regimes typical to thermal analyses.

2. Theoretical model

The proposed model includes several assumptions concerning the main characteristics of the different stages, as stated below. It further suggests that the decomposition rate of a metal hydride particle is limited by hydrogen diffusion through the oxide film surrounding the particle.

(1) A spherical metal hydride particle of a radius R, consisting of a hydride core surrounded by a thin surface oxide film of a thickness δ, is considered (see Fig. 1).
(2) During the initial stage of decomposition, the particle contains a hydride core region β, ($0 < r < R - \delta$), with a constant hydrogen mass fraction C_β. As a result of hydrogen desorption the

hydride core shrinks, creating a region of a solid solution of hydrogen and metal with a constant hydrogen mass fraction $C_{\alpha m}$.

(3) The rate determining process of the hydrogen release from the particle is hydrogen diffusion through the oxide film, since diffusion coefficients within the hydride phase and within the solid solution are larger by several orders of magnitude than those within the oxide [28–30]. As a result it is assumed that hydrogen concentration within both the hydride core and the solid solution is practically uniform. The model addresses a situation where heating rate of the metal hydride particle is sufficiently slow that hydrogen release during the decomposition process does not lead to the oxide layer cracking.
(4) Since $\delta \ll R$, the hydrogen concentration profile within the oxide film is approximately linear.
(5) Hydrogen concentration on the sample external surface is practically zero, since all decomposed hydrogen immediately desorbs to the gas phase.
(6) The diffusion coefficient of hydrogen through the oxide film depends on temperature, $D(T) = D_0 \exp(-E/\Re T)$.
(7) According to phase diagram, the maximum values of hydrogen mass fractions in the hydride core and later in the solid solution are practically independent of temperature, C_β = const, $C_{\alpha m}$ = const.
(8) The instantaneous moving phase boundary of the hydride core and solid solution is defined by ρ: $0 \le \rho \le R - \delta$.
(9) An equilibrium hydrogen concentration within the solid solution exists. The diffusion flux of hydrogen through the oxide film is compensated by hydride core decomposition, so the concentration of hydrogen within the solid solution does not change until the completion of the hydride core decomposition.
(10) The particle is small enough to assume a uniform temperature within the particle.
(11) The rate of change of particle temperature is determined by a heat balance resulting from external heat transfer and endothermic reaction of hydride decomposition.
(12) The surrounding gas pressure is constant.
(13) Spherical symmetry is assumed (like in microgravity).

2.1. Initial conditions

Initial hydrogen mass fractions are defined for the hydride zone, solid solution zone, [there is no solid solution initially] and oxide film zone. The latter is characterized by a linear profile of hydrogen mass fraction: For $r = R - \delta$, $C = C_\beta$, and for $r = R$, $C = 0$.

$$\begin{aligned} &t = 0 \\ &\rho = R - \delta \\ &C = \begin{cases} C_\beta & 0 < r < R - \delta \\ C_\beta - \dfrac{C_\beta}{\delta}(r + \delta - R) & R - \delta < r < R \end{cases} \end{aligned} \tag{1}$$

2.2. Equations system

The total mass flow rate of hydrogen desorption:

$$\dot{m} = \frac{4\pi R^2 D(T) C_\alpha(t) d_\alpha}{\delta} \tag{2}$$

The decomposition balance within the particle at any time in its differential form is (accounting for the assumption that $C_{\alpha m}$ and C_β are unchanged):

$$4\pi\rho^2(t)\frac{d\rho(t)}{dt}C_\beta = 4\pi\rho^2(t)\frac{d\rho(t)}{dt}C_{\alpha m} - 4\pi R^2\frac{C_{\alpha m}D(T)}{\delta} \tag{3}$$

Rearranging Eq. (3), one gets:

$$\frac{1}{3}\frac{d\rho^3(t)}{dt} = -C_{\alpha m}R^2\frac{D(T)}{\delta[C_\beta - C_{\alpha m}]} \tag{4}$$

The last expression is also known as Stephan condition for matter conservation on a moving phase boundary.

The heat balance on the particle includes the particle heating effect $f(T)$ either by the hot ambience gas or due to a constant temperature increase rate, as in TGA, and the endothermic effect of hydrogen desorption as follows ($H_{\beta\to\alpha}$ is defined as positive):

$$\frac{4}{3}\pi R^3\frac{d(T_s\bar{d}\bar{C}_p)}{dt} = -\left(4\pi\rho^2 d_\beta\frac{d\rho}{dt}\right)H_{\beta\to\alpha} + f(T) \tag{5}$$

The average specific heat of the particle is calculated as follows:

$$\bar{C}_p = \frac{\{(4/3)\pi\rho^3 d_\beta C_{p\_\beta} + (4/3)\pi[(R-\delta)^3 - \rho^3]d_\alpha C_{p\_\alpha} + (4/3)\pi(R^3 - (R-\delta)^3)d_{ox}C_{p\_ox}\}}{(4/3)\pi R^3\bar{d}} \tag{6}$$

The average density of the particle is:

$$\bar{d} = \frac{\{(4/3)\pi\rho^3 d_\beta + (4/3)\pi[(R-\delta)^3 - \rho^3]d_\alpha + (4/3)\pi(R^3 - (R-\delta)^3)d_{ox}\}}{(4/3)\pi R^3} \tag{7}$$

d_α and C_{p_α} were calculated by first order interpolation for hydrogen mass fraction within stochiometric hydride and in pure metal.

$$\begin{aligned} d_\alpha &= d_\beta + (C_\beta - C_\alpha)\frac{(d_{metal} - d_\beta)}{C_\beta} \\ C_{p\_\alpha} &= C_{p\_\beta} + (C_\beta - C_\alpha)\frac{(C_{p\_metal} - C_{p\_\beta})}{C_\beta} \end{aligned} \tag{8}$$

The second stage of the process is hydrogen desorption from the solid solution, after the hydride core region diminishes to zero. During this stage there is no source to balance hydrogen diffusion through the oxide film from the solid solution, and hydrogen concentration decreases asymptotically to zero. The differential hydrogen balance equation in this case gets the form:

$$\begin{aligned} &\frac{4}{3}\pi(R-\delta)^3\frac{d(C_\alpha)}{dt} + \frac{4\pi R^2}{\delta}D(T)C_\alpha = 0 \\ &C_\alpha(t = t_*) = C_{\alpha m} \\ &C_\alpha(t = t_{**}) \approx 0 \end{aligned} \tag{9}$$

During this stage the heat balance on the particle includes endothermic transformation of the solid solution to the metal, since the hydride core is totally decomposed:

$$\frac{4}{3}\pi R^3\frac{d(T_s\bar{d}\bar{C}_p)}{dt} = -\left(\frac{4\pi R^2 D(T)C_\alpha d_\alpha}{\delta}\right)H_{\alpha\to M} + f(T) \tag{10}$$

$H_{\alpha\to M}$ is positive and proportional to the hydrogen concentration within the solid solution.

$$\begin{aligned} H_{\alpha\to M} &= H_M - H_\alpha \\ H_\alpha &= H_{\alpha_m} + (C_\alpha - C_{\alpha m})\frac{(H_M - H_{\alpha m})}{0 - C_{\alpha m}} \end{aligned} \tag{11}$$

At this stage the average specific heat $\bar{C}_p$ and average density $\bar{d}$ are expressed as follows:

$$\bar{C}_p = \frac{\{(4/3)\pi[(R-\delta)^3]d_a C_{p\_\alpha} + (4/3)\pi(R^3 - (R-\delta)^3)d_{ox}C_{p\_ox}\}}{(4/3)\pi R^3\bar{d}} \tag{12}$$

$$\bar{d} = \frac{\{(4/3)\pi[(R-\delta)^3]d_\alpha + (4/3)\pi(R^3 - (R-\delta)^3)d_{ox}\}}{(4/3)\pi R^3} \tag{13}$$

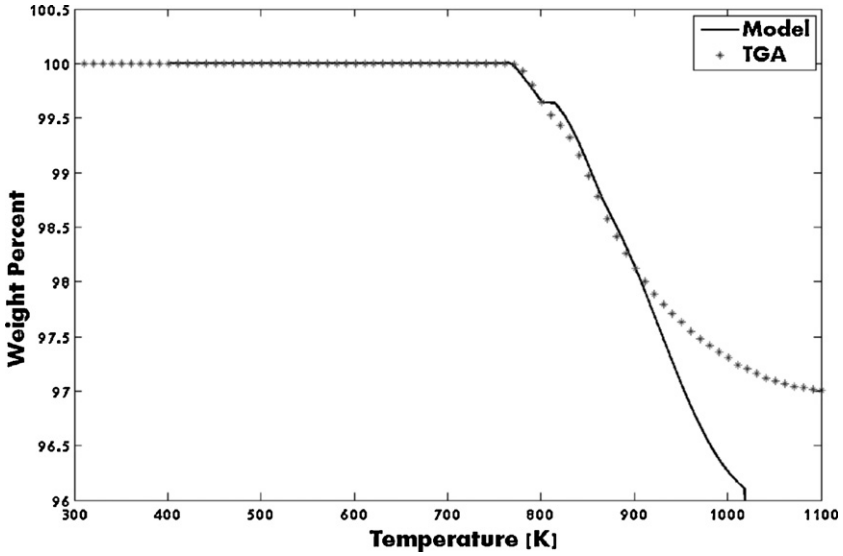

Fig. 2. Model prediction vs. TGA test of titanium hydride decomposition (mean particle size 50 μm). Heating rate 20°/min.

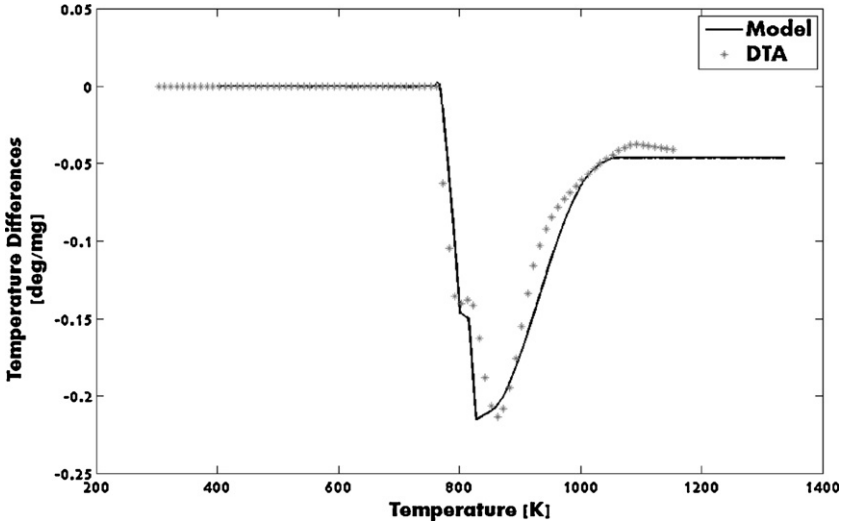

Fig. 3. Model prediction vs. DTA test of titanium hydride decomposition (mean particle size 50 μm). Heating rate 20°/min.

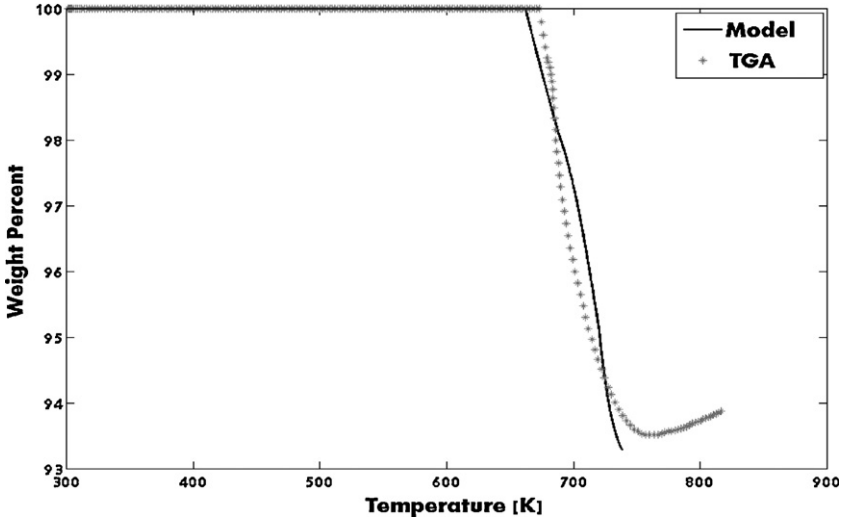

Fig. 4. Model prediction vs. TGA test of magnesium hydride decomposition (mean particle size 0.5 μm). Heating rate 20°/min.

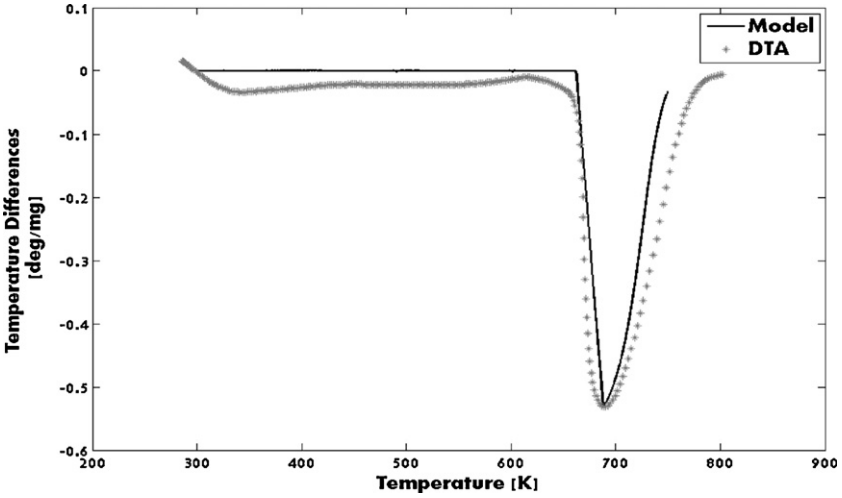

Fig. 5. Model prediction vs. DTA test of magnesium hydride decomposition (mean particle size 0.5 μm). Heating rate 20°/min.

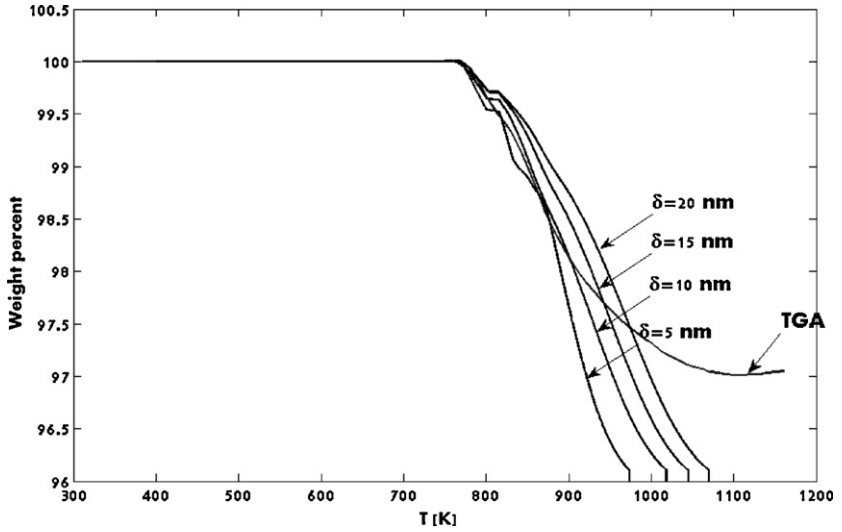

Fig. 6. Model prediction of the influence of initial thickness of oxide layer on titanium hydride decomposition. Mean particle size 50 μm.

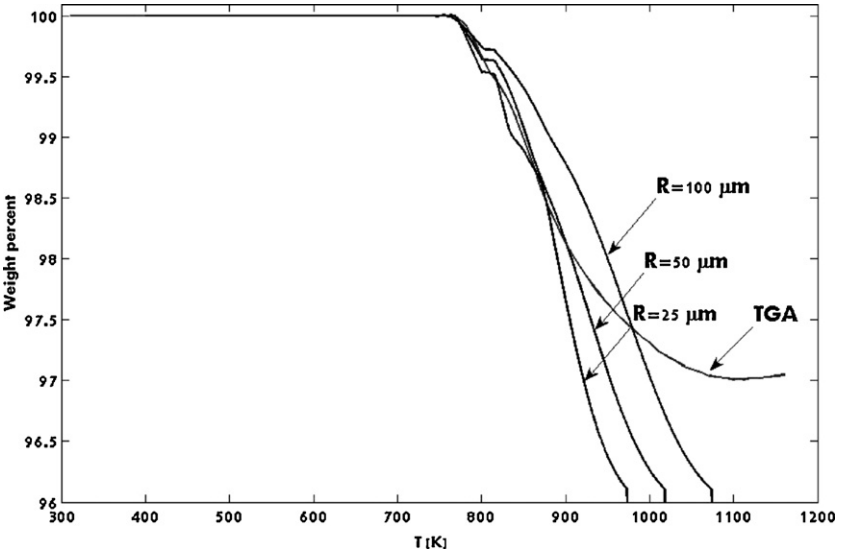

Fig. 7. Model prediction of the influence of titanium hydride particle size on decomposition. Actual mean particle size in TGA test 50 μm.

3. Experimental details

To examine the theoretical model two test series were performed. The thermal decomposition behavior (weight change) of titanium hydride and magnesium hydride was tested in a TGA–DTA apparatus at different heating rates under inert (argon) atmosphere. A constant thickness of oxide layer of 100 Å [33] was assumed. Diffusion coefficient for hydrogen through titanium oxide was taken from [28,34]:

$$D = 10^{-2} \exp\left(\frac{-10,000}{T}\right) \quad [\mathrm{m}^2/\mathrm{s}]$$

Fig. 2 presents TGA test data versus model prediction for titanium hydride decomposition at a heating rate of 20 degrees per minute. Aldrich TiH_2 powder with a mean particle size of 50 μm and purity of 98% was used. Similar results were obtained at other heating rates. A good agreement is demonstrated between the theoretical and experimental results during the initial decomposition stage. Then some deviation occurs, possibly because of traces of oxygen and moisture in the surrounding argon or leaking of traces of air from the ambience into the system, which may cause some oxidation of the metal at high temperatures.

Fig. 3 presents differential temperature analysis (DTA) of titanium hydride decomposition. The decomposition is described as an endothermic process: a negative peak of temperature difference. Close to 800 K there is a small region of temperature plateau, which may indicate phase transition of the material. Similar TGA–DTA tests were performed with magnesium hydride. The sample powder was prepared in the lab by long-time grinding of an as-received magnesium powder under 20 atmospheres of hydrogen. The resulting magnesium hydride powder was of 0.5 μm mean particle size. Figs. 4 and 5 present a comparison between model predictions and experimental results, showing good agreement. There is some deviation in the temperature of the onset of decomposition. It may be caused by inaccurate data on physical properties and their dependence on temperature. For the model calculations, diffusion coefficient for hydrogen diffusion through magnesium oxide was taken from [35]:

$$D = 0.015 \exp\left(\frac{-22,000}{T}\right) \quad [\mathrm{m}^2/\mathrm{s}]$$

Comparative results of TGA for titanium hydride of various particle size and oxide layer thickness are presented in Figs. 6 and 7. As one sees, the model prediction for decomposition rate is only slightly affected by the oxide layer thickness over a range of 5–10 nm. Both particles of 25 and 50 μm size exhibit similar behavior.

4. Summary and conclusions

This work presents a physical–mathematical model for metal hydride decomposition, using the shrinking core approach and considering that hydrogen release rate is limited by hydrogen diffusion through the oxide film surrounding the hydride particle. Experiments of titanium hydride and magnesium hydride decomposition have been conducted. The model results of decomposition under inert atmosphere show a reasonable agreement with TGA–DTA experimental data for both hydrides.

References

[1] M. Ito, D. Setoyama, J. Matsunaga, H. Muta, K. Kurosaki, M. Uno, S. Yamanaka, J. Alloys Compd. 420 (2006) 25–28.
[2] B. Bogdanovic, K. Bohmhammei, B. Christ, A. Reiser, K. Schlichte, R. Vehlen, U. Wolf, J. Alloys Compd. 282 (1999) 84–92.
[3] D. Kyoi, T. Sato, E. Ronnebro, N. Kitamura, A. Ueda, M. Ito, S. Katsuyama, S. Hara, D. Noreus, T. Sakai, J. Alloys Compd. 372 (2004) 213–217.
[4] I. Konstanchuk, K. Gerasimov, J.-L. Bobet, J. Alloys Compd. 509 (2011) S576–S579.
[5] D.A. Sheppard, M. Paskevicous, C.E. Buckley, J. Alloys Compd. 492 (2010) L72–L74.
[6] F.C. Gennari, F.J. Castro, G. Urretavizcaya, J. Alloys Compd. 321 (2001) 46–53.
[7] J.-L. Bobet, C. Even, Y. Nakamura, E. Akiba, B. Darriet, J. Alloys Compd. 298 (2000) 279–284.
[8] J.-L. Bobet, C. Even, J.-M. Quenisset, J. Alloys Compd. 348 (2003) 247–251.
[9] S.K. Dolukhanyan, J. Alloys Compd. 253–254 (1997) 10–12.
[10] L. Li, T. Akiyama, J. Yagi, J. Alloys Compd. 308 (2000) 98–103.
[11] A.G. Aleksanyan, S.K. Dolukhanyan, V.Sh. Shekhtman, J. Huot, O.P. Ter-Galstyan, N.L. Mhatsakanyan, J. Alloys Compd. 509 (2011) S786–S789.
[12] J.F. Fernandez, C.R. Sanchez, J. Alloys Compd. 356–357 (2003) 348–352.
[13] F.J. Castro, G. Meyer, J. Alloys Compd. 330–332 (2002) 59–63.
[14] I. Gabis, E. Evard, A. Voyt, I. Chernov, Y. Zaika, J. Alloys Compd. 356–357 (2003) 353–357.
[15] M.A. Schroeder, J. Propul. Power 14 (1998) 981–991.
[16] E.A. Evard, I.E. Gabis, A.P. Voyt, J. Alloys Compd. 404–406 (2005) 335–338.
[17] M. Avrami, J. Chem. Phys. 7 (1939) 1103–1112.
[18] P. Wang, A.M. Wang, Y.L. Wang, H.F. Zhang, Z.Q. Hu, Scr. Mater. 43 (2000) 83–87.
[19] J. Graetz, J.J. Reilly, J. Phys. Chem. B 109 (2005) 22181–22185.
[20] I.M.K. Ismail, T. Hawkins, Thermochim. Acta 439 (2005) 32–43.
[21] M. Martin, C. Gommel, C. Borkhart, E. Fromm, J. Alloys Compd. 238 (1996) 193–201.
[22] K.C. Chou, Q. Li, Q. Lin, L.J. Jiang, K.D. Xu, Int. J. Hydrogen Energy 30 (2005) 301–309.
[23] G. Gondor, C. Lexcellent, in: Proceedings International Hydrogen Energy Congress and Exhibition, IHEC 2007, Istanbul, Turkey, 13–15 July, 2007.
[24] K.V. Wilson Jr., B.M. Patterson, J. Phillips, J. Nucl. Mater. 374 (2008) 229–240.
[25] T.R. Jensen, A. Andreasen, T. Vegge, J.W. Andreasen, K. Ståhl, A.S. Pedersen, M.M. Nielsen, A.M. Molenbroek, F. Besenbacher, Int. J. Hydrogen Energy 31 (2006) 2052–2062.
[26] H.R.Z. Sandim, B.V. Morante, P.A. Suzuki, Mater. Res. 8 (2005) 293–297.
[27] W. Chen, J. Wang, L. Wang, S. Lu, Trans. Nonferrous Met. Soc. China 17 (2007) 945–948.
[28] G.C. Yu, Phys. Status Solidi (A) 198 (2003) 302–311.
[29] C.K. Coogan, H.S. Gutowsky, J. Chem. Phys. 36 (1962) 110–116.
[30] T. Nishikiori, T. Nohira, Y. Ito, J. Electrochem. Soc. 148 (2001) E127–E132.
[31] F. von Zeppelin, M. Hirscher, H. Stanzick, J. Banhart, Compos. Sci. Technol. 63 (2003) 2293–2300.
[32] S.J. Gao, L.J. Huang, J. Alloys Compd. 293–295 (1999) 412–416.
[33] V.P. Grachukho, M.A. Gurevich, M.I. Savel'ev, Combust. Explos. Shock Waves 14 (1978) 26–31.
[34] G. Stepura, V. Rosenband, A. Gany, in: 47th Israel Annual Conference on Aerospace Sciences, Tel Aviv and Haifa, 21–22 February, 2007.
[35] G. Wu, J. Zhang, Y. Wu, Q. Li, K. Chou, X. Bao, J. Alloys Compd. 480 (2009) 788–793.